NEXUS UNIVERSAL JOURNAL
www.nujournal.in
Volume 2, Issue II: March- April, 2026 (Page:11-24) ISSN: 3108-0367
Received: 30 April , 2026 Published: May 25, 2026

,

Waste Heat Recovery Potential from Internal Combustion Engine Exhaust Gases

Dr. Md Salim Ansari[1] , Ranjan Kumar[2*], Abhishek Anand [3],

Sujit Sinha [4], Suraj Kumar[5], Afzal Hussain[6], Ashish Kumar Mandal[7]

1 Assistant Professor, K K Polytechnic, Govindpur, Dhanbad, Jharkhand, India.

234567 Department of Mechanical Engineering

K K College of Engineering and Management, Govindpur, Dhanbad, Jharkhand, India.

***Corresponding Author-** Ranjan Kumar

Abstract:

Modern internal combustion engines (ICEs) are widely used in transport vehicles, marine, industrial and power generation applications. It is well known that less than a third of the thermal energy input of fuel is transformed into mechanical power, almost 60–70% is wasted as heat through exhaust and cooling systems. This work considers the possibility of utilizing high temperature exhausts, which usually can range from 400°C up to 900°C by modern WHR systems. Experimental investigations and CFD analysis were carried out for different systems such as Organic Rankine Cycles (ORCs), Thermoelectric Generators (TEGs) and combined topping-bottoming cycles. According to results, thermal utilization efficiencies of about 33% were reached by well-designed multi-compartment heat exchangers at peak load conditions. A combined system of shell-and-tube heat exchanger with secondary mechanical recovery achieved improvements in brake thermal efficiency by 0.89% and reduction in brake specific fuel consumption (BSFC) by 5.28g/kWh. This paper presents the thermodynamic, economic and environmental benefits of exhaust waste heat recovery systems.

Keywords: Waste Heat Recovery, Internal Combustion Engine, Exhaust Gases, Thermoelectric Generator

Introduction

Non-renewable energy resources are still strained to meet the demands of an industrialized world, increasing challenges due to energy crises and environmental degradation. The internal combustion engine continues to be the main prime mover in global transportation and localized industry. Thus, improving engine efficiency and minimizing the rate of greenhouse gas production have become priorities among sustainable engineering research pursuits. Deep changes, including high-tech fuel-air atomization and very low tuned combustion (using advanced valve timing) combined with VGT have resulted in optimization of the core in-cylinder process. However, even with those advancements, conventional power generation systems still discard more than half of a fuel's chemical energy to the surrounding environment as low-to-medium-quality waste heat.

A typical thermodynamic energy balance shows that for the fuel chemical input to an engine, only about one third goes into:

Useful work / Brake Power: 25 % –40 %

Cooling System and Lubrication, & Radiation Losses: 35%–40%

Exhaust Gas Enthalpy Content : 30% – 45%

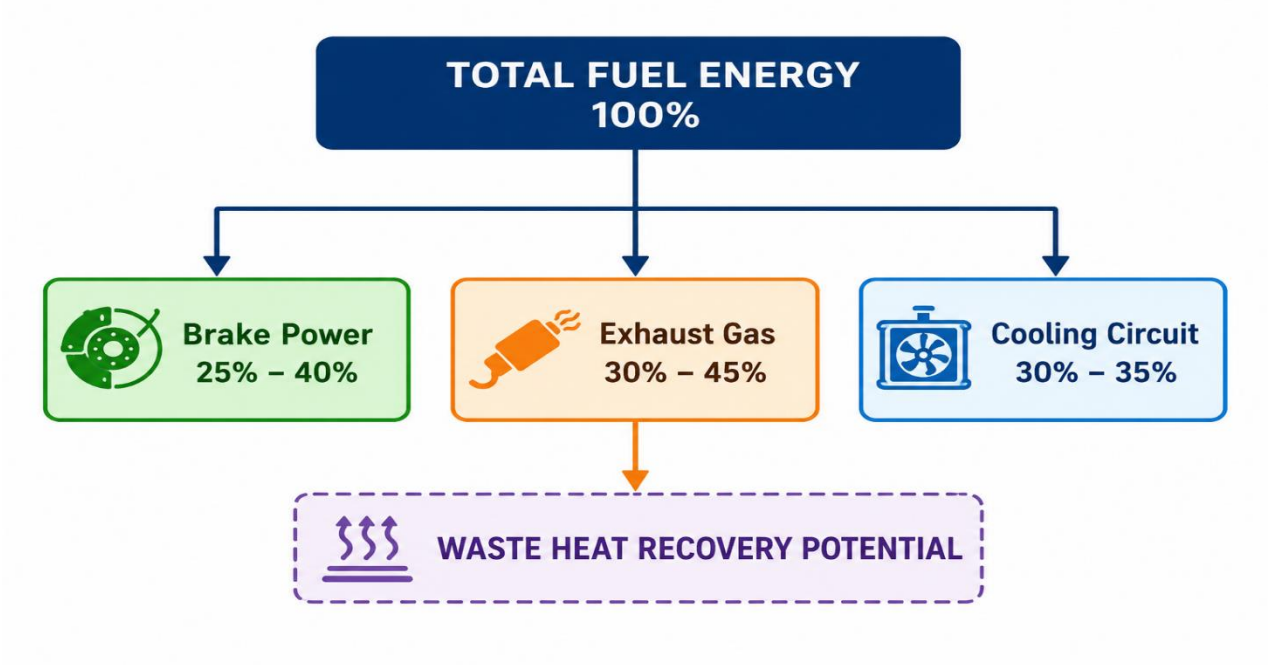

Recycling some of the potential energy present within exhaust gases is a major avenue for energy recovery. While low temperature engine coolant blocks operate at temperatures ranging from approximately 80C to 100C, exhaust gases that immediately exit the engine manifold

have exergy profiles in the range of 400C to 900C. Recovering this energy does not impact core combustion processes and thus establishes a direct pathway toward increased system thermal efficiency.. Prakher Dubey says:

"The recovery and utilization of waste heat not only conserves fuel, usually fossil fuel but also reduces the amount of waste heat and greenhouse gases dumped to environment. It is imperative that serious and concrete effort should be launched for conserving this energy through exhaust heat recovery techniques." (Dubey Prakhar, 2016)

The idea of coupling bottoming recovery plants with ICEs stems from the late 1970s after the world energy geopolitical crises. Camcar's first projects, like Mack Trucks' prototype of a 288-hp commercial vehicle, validated that a verifiable over-the-road test was sufficient to achieve the desired 12.5% real-world reduction in fuel consumption across 450 km of use. Cutting-edge implementations utilize advanced expansion principles, microelectronics and optimized thermodynamic fluids to deliver dependable, scalable frameworks from ocean freight carriers to commercial transport networks.

Literature Review

Vu et al. (2019) investigated exhaust waste heat recovery using a heat exchanger system for marine engine applications. Their study optimized the heat exchanger flow-field using CFD analysis and achieved recovery efficiencies up to 33% at full-load conditions.

Koshy et al. (2015) studied a shell-and-tube heat exchanger coupled with a steam engine for diesel engine waste heat recovery. Their research reported exhaust gas temperatures up to 900.5 K and a maximum recoverable heat energy of approximately 90.4 kW.

Kalariya and Sanathara (2022) reviewed several waste heat recovery technologies and emphasized that nearly 65% of engine thermal energy is lost as waste heat. Their review highlighted thermoelectric generators as promising recovery systems due to their compact size and low maintenance.

Ajwalia (2021) reviewed Organic Rankine Cycle systems and concluded that ORC technology is highly effective for recovering low-grade exhaust heat within the range of 80°C to 350°C.

Moradi et al. (2024) discussed modern waste heat recovery technologies including turbo-compounding, thermoelectric generators, and absorption refrigeration systems.

Methodology and Fundamental Thermodynamic Relations

In order to quantify how much engine waste heat is useful and how much of this can be recovered, a structured mathematical analysis must take place. The heat content loss due to an engine's exhaust gas emission stream can be formulated with the steady-state sensible heat flow relation as follows:

$$Q_{max} = \dot{m}_{ex} \cdot cp_{ex} \cdot (T_{ex,in} - T_{wf,in}) \quad (1)$$

Where:

- $\dot{m}_{wf}$ = mass flow rate of exhaust gas
- $c_{p,ex}$= specific heat capacity of exhaust gas
- $T_{ex,in}$= inlet temperature of exhaust gas
- $T_{wf,in}$= inlet temperature of working fluid

An evaporator bottoming cycle with three major heat transfer processes: liquid preheating (Q 1), latent vaporization (Q2) and superheating (Q3), where the cumulative heat transfer rate is calculated to capture fluid phase changes.

$$Q_1 = \dot{m}_{wf} \cdot cp_{,wf,liq} \cdot (Tsat - Tin) \quad (2)$$

$$Q_2 = \dot{m}_{wf} \cdot h_{fg} \quad (3)$$

$$Q_3 = \dot{m}_{wf} \cdot cp_{,wf,vap} \cdot (T_{out} - T_{sat}) \quad (4)$$

Summing these individual thermal loads yields the maximum cycle heat input:

$$Q_{max} = Q_1 + Q_2 + Q_3 \quad (5)$$

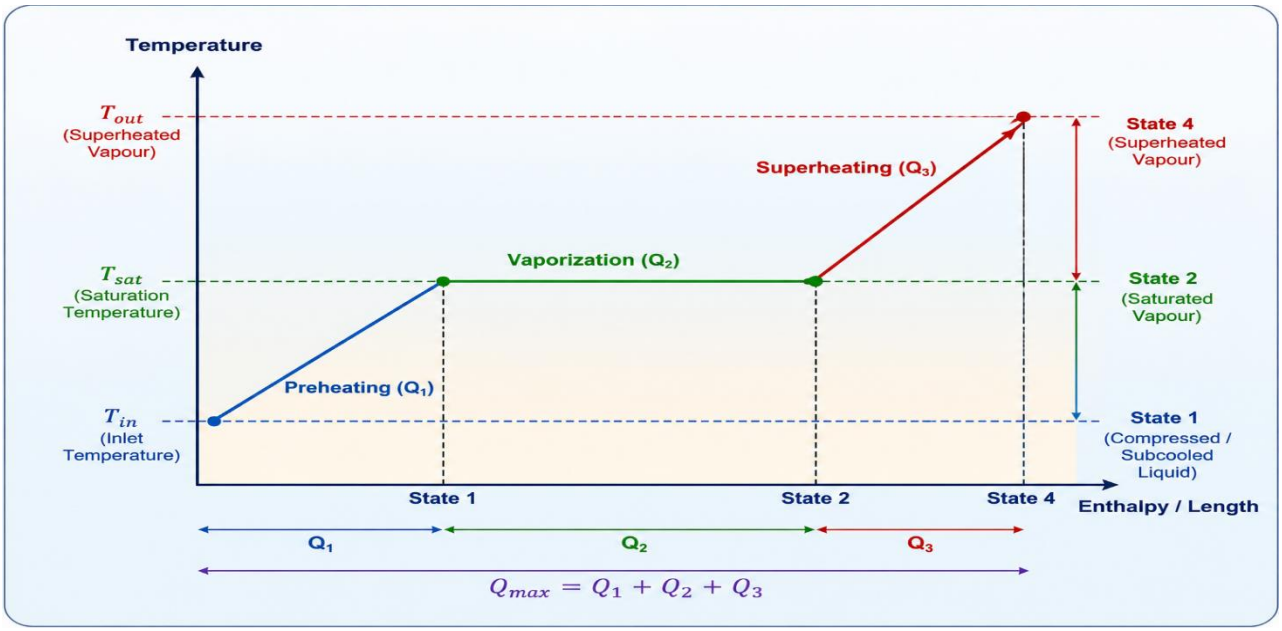

The sizing of the main heat exchange core is done based on the standard Effectiveness-Number of Transfer Units (epsilon-NTU). It sets total area constraints without iterations of calculating the log-mean temperature difference. The dimensionless parameters are defined in the following way:

$$\varepsilon = \frac{Q}{Q_{max}} = f(NTU, C_R) \quad (6)$$

$$NTU = \frac{U \cdot A}{C_{min}} \quad (7)$$

Where U represents the global heat transfer coefficient, A defines the total surface area, and C_{min} is the minimum fluid heat capacity rate.

Case Studies and Mechanical Component Design

his paper describes two separate waste heat recovery validation cases: an ANSYS-CFD fluid design for localized thermal capture and a physical design case optimizing performance metrics of an active vehicle diesel powertrain.

a) Case study A; CFD Flow-field design of small-scale maritime vessels

Quang Khong Vu et al. examined low temperatures waste heat recovery concepts on board small marine platform due to the nature of small vessels leading to very low exhaust mass flows, thus decreasing thermal efficiency. The exhaust properties were modeled with 1D gas dynamics over a range of engine loads, with the thermal source provided by an inline four-cylinder D243 test engine.

Table 1: Exhaust Gas Enthalpy Boundary Conditions vs Engine Load

Engine Load (%)	**Exhaust Temperature (K)**	**Gas Flow Velocity (m/s)**	**Mass Flow Rate (kg/s)**
25%	492%	49%	61.01
50%	602%	55%	60.05
75%	673%	60%	59.30%
100%	733%	70%	58.18%

With these boundary conditions applied, 3D Navier-Stokes simulations in ANSYS Fluent were performed to characterize the flow-field physics for a multi-segmented shell-and-tube heat

exchanger core. The model has tracked heat through the boundaries of the gas, conduction across internal wing fins, and convection into a traction cold seawater distillation loop.

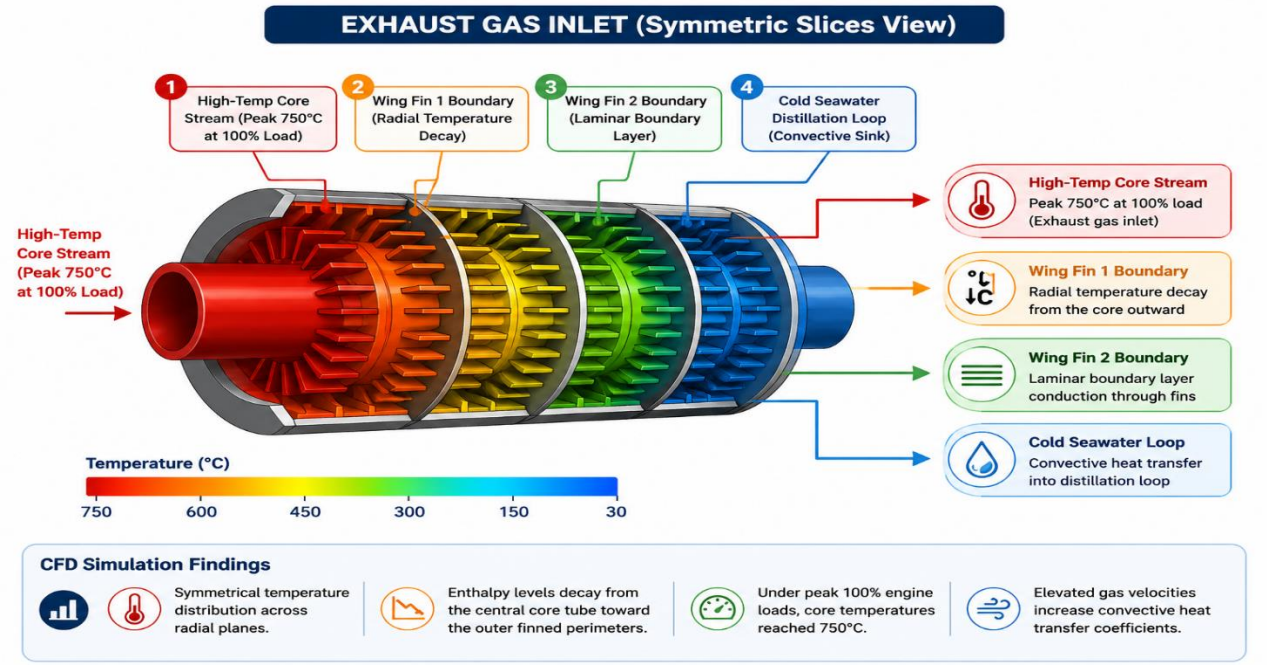

CFD simulations also show that the temperature is symmetrically imposed by radial planes. Enthalpy levels diminished radially outward across the core tube and to the finned perimeters, with this tendency amplified in high engine load conditions. Peak 100% engine loads with core temperatures of 750°C increased the driving temperature differential against seawater sink. In addition, the optimization model also achieved a high waste heat utilization factor (33% at full engine load) with an increase of convective heat transfer coefficients by impairing gas velocities.

b) Case Study B: Co-Generation System for Passenger Vehicles

Alvin P. Koshy et al. You analyzed a commercial vehicle powertrain performance improvement. They developed a counter-flow shell-and-tube heat exchanger connected to an auxiliary uniflow expansion engine that harvested energy from an inline diesel inline four-cylinder power plant of 1,573cc displacement. Diagnostic monitoring confirmed that exhaust gas values reached their maximum at a rated engine speed of 4,000 RPM.

Table 2: Engine Exhaust Operating Parameters vs Rotational Speed

Engine Speed (RPM)	Engine Power Output (kW)	Exhaust Gas Temperature (K)	Exhaust Mass Flow Rate (g/s)
1000	14.9	801.5	18.7

2000	50.2	862.4	83.3
3000	70.8	890.8	59.6
4000	900.5	900.5	108.0

The exhaust gas mass flow rate peaked at 8,000 rpm (0.108 kg/s) which corresponded to a temperature of 900.5K (737 °C). Equation (1) we define the maximum thermal input capacity; you are using a baseline value on the gas specific heat capacity (c_pex}} = 1.185 kJ/kg.K and an initial fluid inlet = 30°.

Q max = 0.108 kg/s x 1.185 kJ/kg. K x (737 - 30) K} = 90.4 kW

Water enters into the high-pressure shell of the recovery plant at 10 bars where its saturation temperature reaches179.9° C. The properties of water from equations (2) to (4) with respect to temperatures can be changed and substituted, i.e. liquid heat capacity (cp,liq = 4.18 kJ/kg·K 7, vapor latent enthalpy (hfg}=2013.6kJ/kg)[8]and superheated vapor heat capacity (Cp,vap)=2.085 kJ/kg·K up to205°C) yields a required secondary fluid mass flow rate(Mwf):

$$Q_1 = \dot{m}_{wf} \times 4.18 \times (179.9 - 30) = 626.58\,\dot{m}_{wf}$$

$$Q_2 = \dot{m}_{wf} \times 2013.6$$

$$Q_3 = \dot{m}_{wf} \times 2.085 \times (205 - 179.9) = 52.34\,\dot{m}_{wf}$$

Equating the combined thermal loads to the maximum heat capacity rate establishes a stable fluid delivery rate of 0.0336 kg/s:

$$90.4\text{ kW} = \dot{m}_{wf} \cdot (626.58 + 2013.6 + 52.34) \Longrightarrow \dot{m}_{wf} = 0.0336\text{ kg/s}$$

Table 3: Sized Heat Exchanger Design Parameters

Mechanical Property Profile	Sized Engineering Value
Global Heat Exchanger Effectiveness (€)	76.3%
Total Heat Transfer Area (A)	18.87m^2
Internal Tube Pitch Layout	1-inch Square Configuration
Tube Dimensional Boundaries	ID: 12.2 mm
Outer Shell Diameter Bounds	ID: 438.15 mm
Total Fluid Tubes Enclosed	150 Channels

Internal Fluid Passes / Baffles	6 Passes

To verify the mechanical integrity of the components under high-temperature and high-pressure conditions, 3D structural designs were developed in CATIA and analyzed via finite element analysis (FEA) in ANSYS.

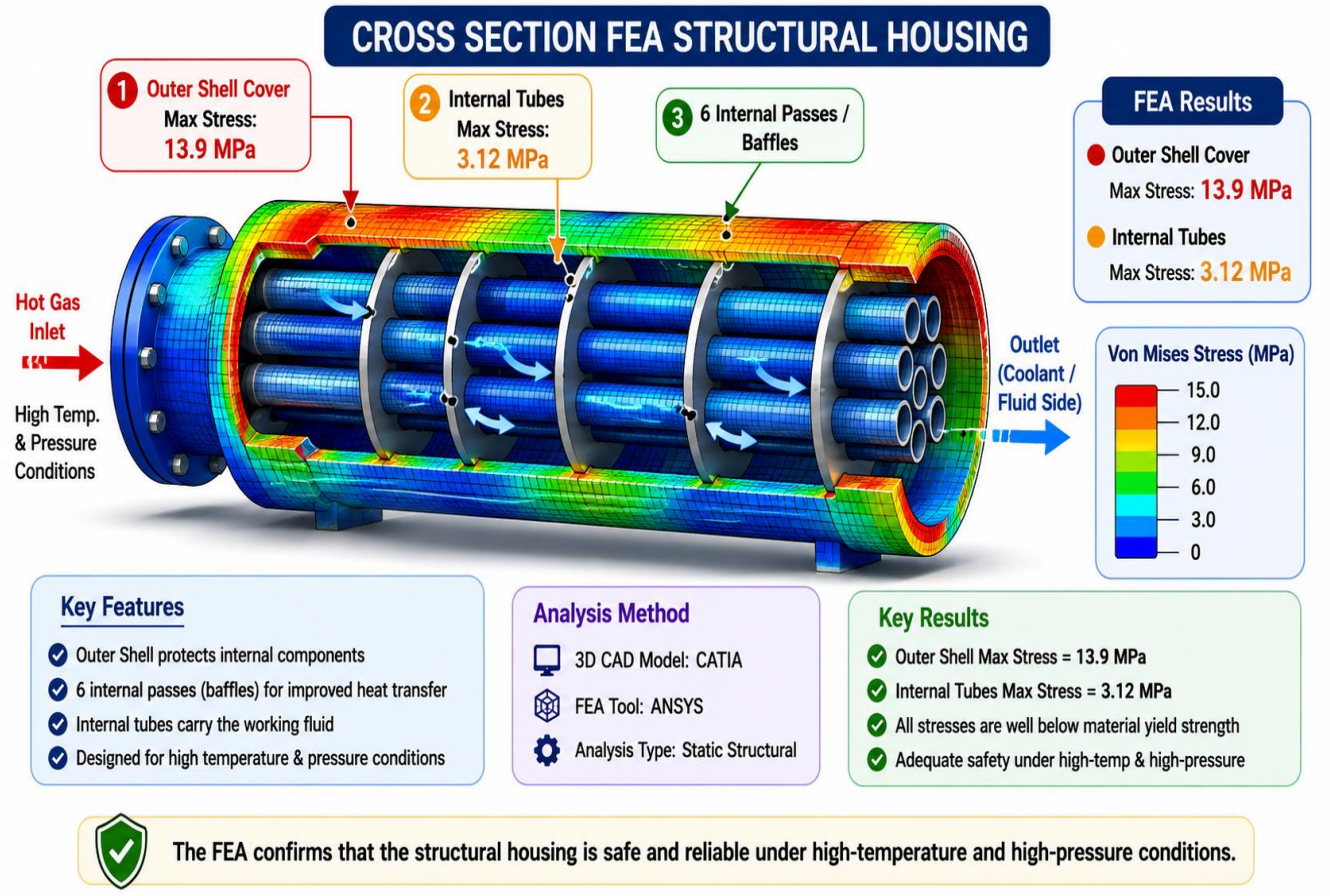

The structural analysis confirmed that localized mechanical stresses remained well below the yield strengths of the selected materials. The safety factors (SF) for the critical components were calculated as follows:

$$SF_{\text{shell cover}} = \frac{250\ \text{MPa}}{13.9\ \text{MPa}} = 17.98$$

$$SF_{\text{outer shell}} = \frac{250\ \text{MPa}}{28.26\ \text{MPa}} = 8.84$$

$$SF_{\text{internal tubes}} = \frac{15\ \text{MPa}}{3.126\ \text{MPa}} = 4.79$$

These conservative metrics confirmed the structural safety of the assembly under high thermal loads, preventing failure from mechanical stress or fatigue.

System Optimization and Bottoming Fluids Selection

- Wet Fluids (Negative Slope): Like water (H2O) that expand and form liquid droplets and can only operate with enough superheating to not erode the turbine blades.
- Dry Fluids (Negative/Isentropic Slope): e.g., benzene that stays superheated during expansion and protects turbo-expander parts
- Isentropic Fluids (Vertical Slope): Including R134a and R11 fluids, where expansion closely follows the saturated vapor line to allow for full evaporation and avoid any two-phase condensate at the Cold Plate, which would require complex reheating devices to achieve an overall thermal efficiency improvement without adding substantial cost.

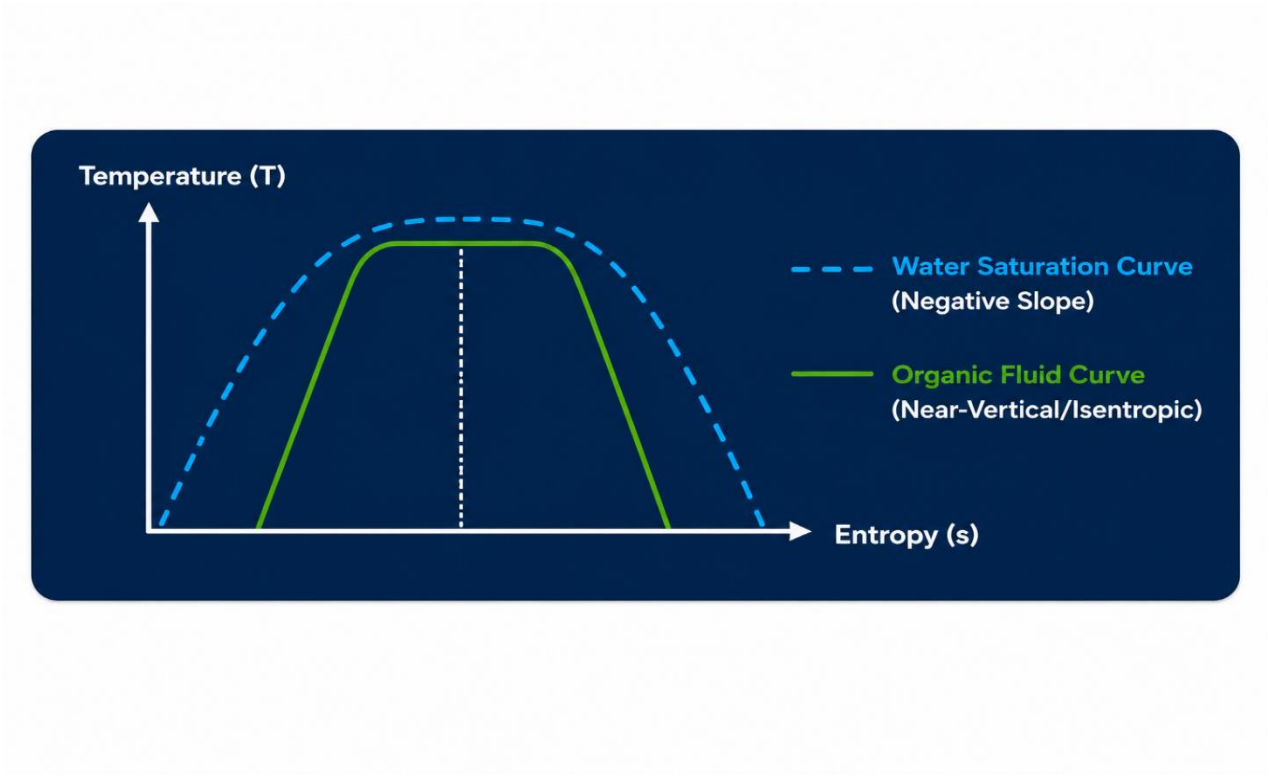

Table 4: Thermophysical Properties of Working Fluids

Parameter Profile	**Water (H2 O)**	**Ammonia (NH3)**	**Benzene (C6H6)**	**R134a**	**R12**	**R11**
Molecular Weight	18	17	78.14	102	121	137
Saturated Curve Slope	Negative	Negative	Positive	Isentropic	Isentropic	Isentropic

Turbine Enthalpy Drop (kJ/kg)	1570 – 900	725 – 70	120 – 230	55 – 22	43 – 20	80 – 40
Max Stability Limit (K)	None	750	600	450	450	420–450
Sized Expander Stages	Multi-Stage	Multi-Stage	Single-Stage	Single-Stage	Single-Stage	Single-Stage
Critical Temperature (K)	647	405.2	562.3	374.14	385	471

Water has great turbine enthalpy drop but a low condensing pressure (less than 100 mbar absolute), which makes the cycle more vulnerable to leaks of atmospheric air. In contrast, most low-temperature organic fluids such as R134a and R245fa condense outside a vacuum above atmospheric pressure, where complex vacuum systems are not required and single-stage expansion architectures become feasible.

This thermophysical optimization is accomplished by the need of producing candidate fluids that offer high thermal conductivity and low dynamic viscosity in a way that optimizes heat exchange performance. This leads to minimized physical size and weight of the heat exchanger core due to notably high thermal conductivity, whereas a low viscosity profile ensures that fluid circulation requires minimal mechanical pumping effort.

Performance Results and Environmental Impact Analysis

Implementing the co-generation plant in Case Study B led to significant gains in performance across the system as a whole. Linking the output of the expansion engine to main crankshaft needless internal friction losses through power and idle strokes

Improvement in Engine Performance

a) Variation in Thermal Efficiency

Thermal efficiency , η_{bth} of the IC engine: $= 37.3\%$

$$\text{But,} \eta_{bth} = \frac{\text{Brake Power (bp)}}{(\text{Mass of Fuel/sec}) \times (\text{Calorific Value of Diesel})}$$

We also know:

$$\text{Brake Power} = 80 \text{ kW}$$

$$(\text{Mass of Fuel/sec}) \times (\text{Calorific Value of Diesel}) = 214.477 \text{ kW}$$

New brake power:

$$\text{New Brake Power} = \text{bp of IC engine} + \frac{\text{bp of steam engine}}{2}$$

$$= 80 + 1.91895$$

$$= 81.91895 \text{ kW}$$

New thermal efficiency:

$$\eta_{bth} = \frac{81.91895}{(\text{Mass of Fuel/sec}) \times (\text{Calorific Value of Diesel})}$$

$$= \frac{81.91895}{214.477}$$

$$= 38.19\%$$

Increase in thermal efficiency:

$$38.19 - 37.30 = 0.8947\%$$

b) Variation in Brake Specific Fuel Consumption

Brake specific fuel consumption (BSFC) of the IC engine:

$$\text{BSFC} = 225 \text{ g/kWh}$$

But, $\text{BSFC} = \frac{\text{Fuel Consumption per Unit Time}}{\text{Brake Power}}$

Fuel consumption for unit time at 80 kW: $= 18000$ g/hr

New BSFC: $\text{BSFC}_{new} = \frac{18000}{81.91895}$

$$= 219.72 \text{ g/kWh}$$

Decrease in BSFC: $225 - 219.72 = 5.28$ g/kWh

As a result, at the international level these savings in fuel translate into a lowered discharge of exhaust gas emissions of carbon monoxide (CO), hydrocarbons (HC), NOx and PM. The latter is effective enough to reduce cumulative tailpipe emissions of carbon monoxide and carbon dioxide by as much as 7% and 3.6%, respectively, at an industrial scale—using heat exchangers during cold starts to accelerate the warm-up of lubricant.

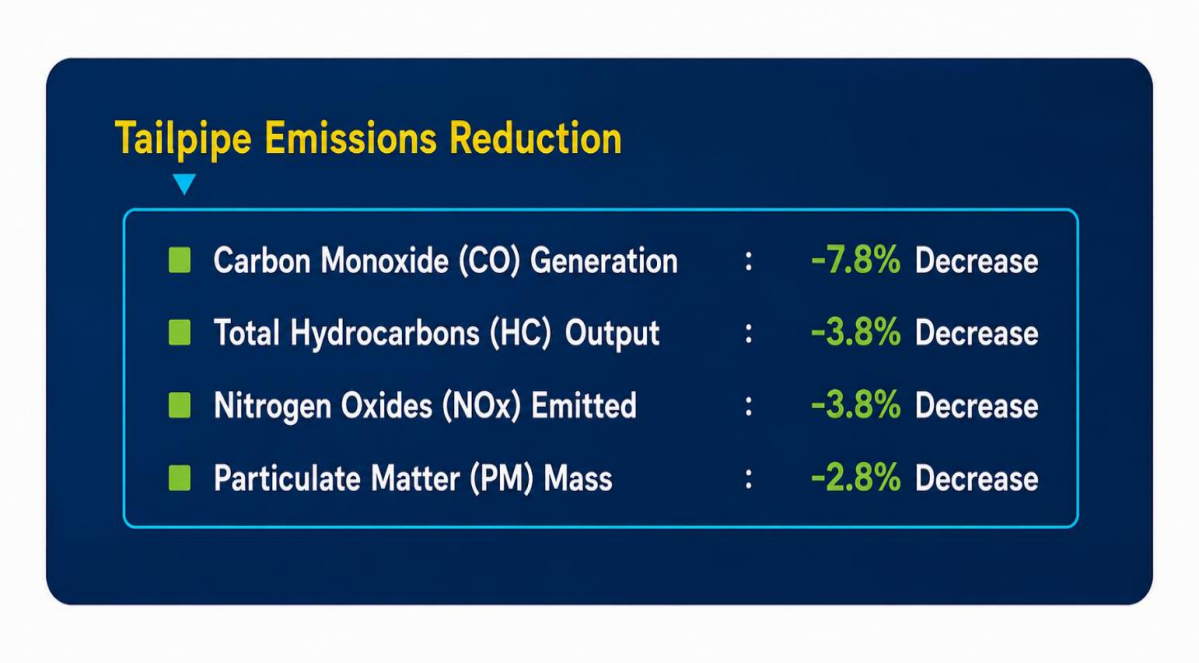

From an economic perspective, waste heat recovery systems require balancing higher upfront manufacturing costs against long-term fuel savings. The initial capital expenditures include high-pressure shell fabrications, specialized fluid connections, and precision multi-stage expansion turbines. However, in heavy-duty shipping and long-haul commercial transport applications with high-capacity factors, the reduction in fuel costs offsets the initial system investment, making the recovery plant highly profitable over its operational lifetime.

Result and Discussion

Economically, waste heat recovery systems come with higher manufacturing costs but offset this cost through fuel savings over the life of the unit. Early capital expenditures include high-pressure shell fabriions, specialized fluid connections and multi-stage expansion turbines with a series of precision engineered blades. But in high-capacity factor applications such as heavy-duty shipping and long-haul commercial transportation, the fuel savings far exceed any initial system investment, rendering a highly profitable recovery plant for its entire lifetime.

Result and Discussion

Engineering restraints, thermodynamic performances, fluid selections and the structural safe design margins for vehicular waste heat recovery systems were explored in this paper. The experimental and computational data shows that capturing high-exergy exhaust gas streams is a direct, highly effective route to engine efficiency gains without changing the core combustion parameters.

Key engineering findings from this research include:

- Building on this knowledge, new advanced multi-compartment heat exchangers optimized through computational fluid dynamics (CFD) have been used to couple efficiencies of 33% thermal utilization factors when operating at full engine load.
- This study incorporated a counter-flow shell-and-tube heat transfer loop with an auxiliary mechanical expander yielding a net power increase of 1.92 kW, increasing the brake thermal efficiency from 37.30% to 38.19%.
- This reclaimed thermal energy reduced brake specific fuel consumption by 5.28 g/kWh, translating into a corresponding reduction in tailpipe emissions of carbon monoxide, hydrocarbons and greenhouse gases.
- Finite element analysis (FEA) validated that structural components feature conservative factor-of-safety margins (4.79–17.98) under peak thermal stresses confirming mechanical viability of the design

Conclusion

Waste heat recovery plants provide an unprecedented level of efficiency and environmental benefit for heavy duty shipping, marine transport and continuous power generation applications, but face high upfront material costs associated with structural integration packaging in the small passenger vehicle segments. Further developments for high temperature isentropic organic fluids, compact micro-channel heat exchangers, and low-maintenance expansion turbines will more commercially enable these systems to bring the transport sector a step closer to modern energy sustainable choices.

References

- Ajwalia, K. (2021). Comprehensive review of ORC's application: Waste heat recovery system in IC engine. In *Proceedings of the 46th Workshop on Geothermal Reservoir Engineering* (SGP-TR-218). Stanford University.
- Domingues, A., Santos, H., & Costa, M. (2013). Analysis of vehicle exhaust waste heat recovery potential using a Rankine cycle. *Energy, 49*, 71–85.
- Dubey, P. (2016). Waste heat recovery systems for internal combustion engines. *International Journal of Scientific Progress and Research, 20*(1), 26–29.
- Fu, J., Liu, J., Yang, Y., Ren, C., & Zhu, G. (2013). A new approach for exhaust energy recovery of internal combustion engines. *Applied Energy, 112*, 784–792.

- Heywood, J. B. (2018). *Internal combustion engine fundamentals* (2nd ed.). McGraw-Hill Education.
- Jadhao, J. S., & Thombare, D. G. (2013). Review on exhaust gas heat recovery for I.C. engine. *International Journal of Engineering and Innovative Technology*, *2*(12), 93–100.
- Kalariya, K., & Sanathara, M. (2022). Scope of waste heat recovery in internal combustion engines: A review. In *Proceedings of the International Conference on Science, Engineering and Technology (ICSET 2022)* (pp. 519–526). RK University.
- Kern, D. Q. (1950). *Process heat transfer*. McGraw-Hill.
- Koshy, A. P., Johnson, J. E., Bijeesh, P., Jose, B. K., & Krishnan, K. N. (2015). Exhaust gas waste heat recovery and utilization system in IC engine. *International Journal for Innovative Research in Science & Technology*, *1*(11), 392–400.
- Kothandaraman, C. P., & Subramanyan, S. (2014). *Heat and mass transfer data book*. New Age International Publishers.
- Moradi, J., Andwari, A. M., Könnö, J., Gharehghani, A., & Pesyridis, A. (2024). Waste heat recovery technologies in modern internal combustion engines. *Future Energy, 3*(3), 49–54.
- O'Halloran, S., & Rodrigues, M. (2012). *Power and efficiency measurement in a thermoelectric generator*. American Society for Engineering Education.
- Orr, B., Akbarzadeh, A., Mochizuki, M., & Singh, R. (2016). A review of car waste heat recovery systems utilising thermoelectric generators and heat pipes. *Applied Thermal Engineering, 101*, 490–495.
- Sprouse, C., III, & Depcik, C. (2013). Review of organic Rankine cycles for internal combustion engine exhaust waste heat recovery. *Applied Thermal Engineering, 51*(1–2), 711–722.
- Vu, Q. K., Minh, D. V., Duy, T. N., Minh, T. P., & The, L. N. (2019). A study of exhaust waste heat recovery in internal combustion engines. *IOP Conference Series: Materials Science and Engineering*, *507*(1), Article 012028.
- Wang, P., Wang, B. L., & Li, J. E. (2019). Temperature and performance modeling of thermoelectric generators. *International Journal of Heat and Mass Transfer, 143*, 118564.